Contents lists available at ScienceDirect

Behavioural Brain Research

Association between structural brain features and gene expression by weighted gene co-expression network analysis in conversion from MCI to AD

Xuwen Wang, Kexin Huang, Fan Yang, Dihun Chen, Suping Cai *, Liyu Huang *

School of Life Sciences and Technology, Xidian University, Xi'an, Shaanxi, 710071, PR China

ABSTRACT

Alzheimer's disease (AD) is a neurodegenerative disease. Mild cognitive impairment (MCI) represents a state of cognitive function between normal cognition and dementia. Longitudinal studies showed that some MCI patients remained in a state of MCI, and some developed AD. The reason for these different conversions from MCI remains to be investigated. 180 MCI participants were followed for eight years. 143 MCI patients maintained the MCI state (MCI_S), and the remaining thirty-seven MCI patients were re-evaluated as having AD (MCI_AD). We obtained 1,036 structural brain characteristics and 15,481 gene expression values from the 180 MCI participants and applied weighted gene co-expression network analysis (WGCNA) to explore the relationship between structural brain features and gene expression. Regulating mediator effect analysis was employed to explore the relationships among gene expression, brain region measurements and clinical phenotypes. We found that 60 genes from the MCI_S group and 18 genes from the MCI_AD group respectively had the most significant correlations with left paracentral lobule and sulcus (L.PTS) and right subparietal sulcus (R.SubPS) thickness; CTCF, UQCR11 and WDR5B were the mutual genes between the two groups. The expression of CTCF gene and clinical score are completely mediated by L.PTS thickness, and the UQCR11 and WDR5B gene expression levels significantly regulate the mediating effect pathway. In conclusion, the factors affecting the different conversions from MCI are closely related to L.PTS thickness and the CTCF, UQCR11 and WDR5B gene expression levels. Our results add a theoretical foundation of imaging genetics for conversion from MCI to AD.

1. Introduction

Alzheimer's disease (AD) is a neurodegenerative disease and the most common cause of dementia [1]. Mild cognitive impairment (MCI) represents the transitional stage from normal cognition to dementia [2]. A meta-analysis of 41 studies that followed MCI patients for > 3 years found that the annual conversion rate to dementia was ~5 % to 10 % [3]. In other words, in a random sample of 100 MCI patients, ~5 to 15 will convert to dementia within the first year. Regardless of the true rate, MCI remains a reliable predictor for future conversion to dementia. Therefore, it is necessary to study the specific risk factors for the progression from MCI to AD, such as imaging and genetic factors [4]. The design of this study was based on such a research problem.

Structural magnetic resonance imaging (sMRI) biomarkers of MCI or AD are an active research area. A wide range of biomarkers have been proposed and investigated [5]. Cortical thickness is a sensitive biomarker that can be used to track the cognitive and neuropathological symptoms of dementia, and cortical thinning may be a marker of AD progression [6]. Moreover, genetic factors, such as the apolipoprotein E (APOE) gene, which is one of the greatest risk factors for this disease, may play an important role in the development of AD [7]. Prevailing evidence suggests that CTCF is pivotal for the up-regulation of amyloid precursor protein (APP) expression during synaptogenesis in primary neurons [8]. Liu et al. [9], have identified that UQCR11 plays a role in the biological process of mitochondrial dysfunction in AD. Lambert et al. [10], detected 19 loci that reached genome-wide significance, of which 11 were associated with pathogenic factors of AD. Genetic and genomic studies offer insight into many additional genetic risk loci involved in the genetically complex nature of AD. A prior study identified four novel genes associated with cortical thickness in AD [11]. Is there a relationship between structural brain features and gene expression in the pathologic mechanism of AD?

Weighted gene co-expression network analysis (WGCNA) is a systems biology method for describing the correlation patterns between brain MRI traits and genetic features and has been successfully applied in various biological contexts, such as the analysis of brain imaging data, AD, aging and other neurodegenerative diseases [12–15]. WGCNA corresponds to a data reduction method and an unsupervised classification method that relies on the assumption that highly correlated genes within a module are involved in common biological processes [12]. This method not only focuses on differentially expressed genes (DEGs) but also combines genes with phenotypic and behavioral traits of interest. It emphasizes the use of integrating massive genes to phenotypes and behavioral traits instead of studying the effects of a single gene [16]. It can also be used to identify candidate biomarkers or therapeutic targets. Soleimani Zakeri et al. [17], applied the WGCNA method to identify several novel gene biomarkers of AD at different stages. Sato et al. [18], used WGCNA to detect coordinated modules of brain atrophy and demonstrated their longitudinal extension along the clinical course of AD progression. This evidence suggests that WGCNA is a suitable method for building a bridge between aberrant gene expression and sample features and provides insights into a systematic signaling network that may be associated with phenotypes of interest. Therefore, we applied this method to investigate the relationship between gene expression, brain measures and the clinical phenotype of MCI with different conversions and preliminary explored the reason for conversion from MCI to AD.

Here, we ask three specific questions: 1) Which brain features are associated with the conversion from MCI to AD? 2) Which genes are associated with this conversion? 3) What is the association between this brain features and genes? We address these questions by combining magnetic resonance imaging with gene expression data in MCI. The hypothesis is that there is an association between structural brain features and gene expression in patients with conversion from MCI to AD. In the current study, 180 MCI participants who were longitudinally followed for eight years were enrolled. In total, 37 MCI participants developed AD (MCI_AD). The remaining 143 participants remained in the MCI state (MCI_S). We identified the DEGs and morphological features of the brain cortex between the two groups. A co-expression network was constructed by using WGCNA to explore the relationship between structural brain features and gene expression levels. Then, key modules and hub genes associated with these two groups were identified. Correlation analysis and regulating mediator effect analysis were performed to investigate the relationships among gene expression, brain region measurements and clinical phenotypes. We intended to lay a theoretical foundation for the factors of MCI conversion to AD.

2. Materials and methods

2.1. Sample dataset

The data we used for our study is from the Alzheimer's Disease Neuroimaging Initiative (ADNI) database (adni.loni.usc.edu). ADNI is devoted to the identification and understanding of features that mark AD progress. The database includes clinical data, magnetic resonance imaging (MRI) data, genetic data and so on. We tracked 190 (after quality control, 180 participants are used in this study) participants of MCI about eight years. After the late visit records (June 2019), we find that 143 participants who maintained MCI (MCI_S) and 37 MCI participants turned into AD (MCI_AD). The specific time of conversion in 37 MCI participants is shown in Supplementary Table S1. We obtained those clinical phenotype data, sMRI data and gene expression data in the baseline time (tracking start time, May 2011).

2.2. Ethical statement

We confirmed that all procedures performed in this study involving human participants were in accordance with the ethical standards of the ADNI consortium Ethics Committee and with the 1964 Helsinki declaration and its later amendments or comparable ethical standard. Written informed consent was obtained from all participants or surrogates (adni.loni.usc.edu).

2.3. Quality control

One of the most common artefacts in structural brain imaging is motion-induced artefacts. Blumenthal, J.D. et al., [19] and Pardoe et al. [20], discussed motion and morphometry in clinical and nonclinical populations. The ADNI database identified the motion in a raw anatomical image by visual inspection. Then, we applied automated Brain Images Database Structure (BIDS) apps, which can assess raw anatomical MRI scans for quality and output quantitative measurements [21]. After this step, 10 subjects (4 MCI_S, 6 MCI_AD) were removed.

2.4. sMRI data processing

T1-weighted MRI preprocessing included segmentation, normalization and modulation. The detailed steps were published in our previous paper [22]. Then, the brain was divided into 148 regions, and the following seven brain measures were extracted using FreeSurfer (http://www.freesurfer.net/): volume, thickness, area, mean curvature, Gaussian curvature, folding degree, and curving degree. Two-sample T tests (sex, age and whole brain volume as a covariate) were used to obtain the differences in these measures of 148 brain regions.

2.5. Gene expression data processing

Detailed microarray gene expression profiling of ADNI participants is shown on the ADNI website (https://ida.loni.usc.edu/pages/access/geneticData). Samples were randomized to plates, checked to ensure balanced sex and diagnostic traits, and hybridized to the Affymetrix Human Genome U219 array plate. Array hybridization, washing, staining, and scanning were carried out on an Affymetrix GeneTitan system. The quality of gene expression data, including sample quality and hybridization and overall signal quality, was analyzed using Affymetrix Expression Console software and Partek Genomic Suite 6.6 according to standard QC criteria provided by each software package. Raw expression values obtained directly from CEL files were preprocessed using the robust multi-chip average (RMA) normalization method. The Affymetrix HG U219 Array contains 530,467 probes for 49,293 transcripts. All Affymetrix U219 probe sets were mapped and annotated with reference to the human genome (hg19). We downloaded the original gene expression data, which contained 32,417 genes. We averaged the corresponding expression values of the repeat genes and then obtained the expression data of 15,481 genes. DEGs were detected between the MCI_S and MCI_AD groups based on a two-sample T test (sex, age and whole brain volume as a covariate). All the statistical analyses were carried out using IBM SPSS Statistical 22. Multiple comparisons correction was applied ($p < 0.05$). DEGs and differentially regions in brain measures were used to construct a co-expression network.

2.6. WGCNA

To explore the potential relationship between DEGs and the differentially brain regions, the WGCNA package in R software was used to construct a gene co-expression network to identify meaningful gene modules. A total of 143 samples from the MCI_S group and 37 samples from the MCI_AD group were subjected to WGCNA, which used 649 DEGs and 26 differentially brain regions. Eventually, the highly co-expressed gene modules were inferred from the DEGs. DEGs were divided into different modules with different colors. We constructed associations between gene modules and brain regions and used the R package to visualize the module results. Gene expression values were extracted from the most significant correlation module for further

analysis.

2.7. Enrichment analysis

Functional enrichment analysis was carried out using genes from the most significant correlation co-expression modules of these two groups. The genetic information was mapped to the associated Gene Ontology (GO) terms and Kyoto Encyclopedia of Genes and Genomes (KEGG) pathways using the Metascape tool (http://metascape.org/) [23].

2.8. Identification of hub genes

The highest intramodular connectivity (highest relationship with certain clinical traits and module eigengenes) of genes was identified by the WGCNA algorithm as a hub gene of the module. The connectivity between genes was measured by the absolute value of Pearson's correlation. Gene significance (GS) is defined as the relationship between gene expression and certain clinical traits. Module membership (MM) represents the correlation between gene expression and module eigengenes. Genes with high GS and MM were considered the most important in the modules were tightly associated with clinical traits. As such, genes with high GS and MM can be used for subsequent analysis.

2.9. Correlation analysis

We extracted the expression values of the hub genes, the measure values of corresponding brain regions, and the clinical phenotype scores from the MCI_S and MCI_AD groups. Then, we performed Pearson correlation analysis among those values using IBM SPSS Statistical 22. We selected the genes with significant correlations for further explanatory analysis.

2.10. Regulating mediator effects analysis

Mediating effect analysis and regulating mediator effect analysis were performed to explore the relationships among the gene expression values, the brain region measures and the clinical phenotypes. Whether cortical thickness in the L.PTS mediates the relationship between the gene expression value and clinical score and whether the moderating effect is regulated by the one of the two genes were assessed. The pathway of mediator effects was defined as $X => M => Y$, where X is the gene expression (independent variable), M is the brain region measure (mediating variable), and Y is the clinical phenotype (dependent variable). Regulating variable Z regulated the mediator effects in the pathways of $X => M$ or $M => Y$.

3. Results

3.1. Demographics and clinical results

Age and sex were matched between the MCI_S and MCI_AD groups. Compared with the MCI_S group, the MCI_AD group had significantly lower clinical scores including MMSE, ADNI_MEM, ADNI_EF and ADNI_LAN scores, and higher ADAS and FAQ scores. There was no significant difference in the ADNI_VS and CDR scores. Demographic information is shown in Table 1.

3.2. Identification of differentially brain regions and DEGs between the MCI_S and MCI_AD groups

Seven brain measures were extracted: volume, thickness, area, mean curvature, Gaussian curvature, folding degree, and curving degree. Each brain measure contained 148 brain regions. Therefore, we obtained 7*148 features from each participant. After statistical analysis, twenty-six features of the corresponding brain region showed significant differences ($p < 0.0001$, FDR correction), including the thickness of the left

Table 1
Demographic information.

Clinical characteristic	MCI		p values
	MCI_S (n = 143)	MCI_AD (n = 37)	
Sex (M/F)	143 (80/63)	37 (26/11)	0.114
Age	71.41 ± 7.59	73.35 ± 7.19	0.162
MMSE	28.31 ± 1.57	27.57 ± 1.82	0.014*
ADAS	12.48 ± 5.45	20.14 ± 6.00	0.000**
ADNI_MEM	0.61 ± 0.59	−0.06 ± 0.69	0.000**
ADNI_EF	0.60 ± 0.86	0.05 ± 1.03	0.001**
ADNI_LAN	0.55 ± 0.67	0.03 ± 0.93	0.000**
ADNI_VS	0.05 ± 0.69	−0.02 ± 0.83	0.621
CDR	0.05 ± 0.00	0.05 ± 0.00	1
FAQ	1.80 ± 2.96	5.35 ± 4.61	0.000**

Data are shown as the mean ± std, and p values were obtained from two-sample T tests and 5000 bootstrapping tests (**: $p < 0.01$; *: $p < 0.05$). MCI_S: stable MCI; MCI_AD: conversion from MCI to AD; MMSE: Mini-Mental State Examination; ADAS: Alzheimer's Disease Assessment Scale: 13 items of word recall, commands, construction, delayed word recall, naming, ideational praxis, orientation, word recognition, recall instructions, spoken language, word finding, comprehension, and number cancellation; ADNI_MEM: composite score for memory in the ADNI database. ADNI_EF: composite score for executive functioning in the ADNI database; ADNI_LAN: composite score for language in the ADNI database; ADNI_VS: composite score for visuospatial functioning in the ADNI database; CDR: Clinical Dementia Rate; FAQ: Functional Activities Questionnaire.

paracentral lobule and sulcus (L.PTS) and the thickness of the right subparietal sulcus (R.SubPS). Detailed information on the twenty-six features is provided in Supplementary Table S1.

A total of 649 DEGs were identified between the MCI_S and MCI_AD groups based on the two-sample T test ($p < 0.05$, FDR correction).

3.3. WGCNA results

For the MCI_S group, we constructed a WGCNA network using an unsigned type of adjacent matrix and topological overlap matrix (TOM), the correlation coefficient of the Pearson algorithm, a power β of 6 (Supplementary Fig. S1(A)), a minimal module size of 10 and a merge cut height of 0.15. This analysis revealed six modules: green, yellow, blue, turquoise, brown and red (Supplementary Fig. S2(A)). For the MCI_AD group, we also constructed a WGCNA network using an unsigned type of adjacent matrix and TOM, the correlation coefficient of the Pearson algorithm, a power β of 9 (Supplementary Fig. S1(B)), a minimal module size of 8 and a merge cut height of 0.15. This analysis revealed six modules: green, turquoise, blue, brown, red and yellow (Supplementary Fig. S2(B)). Genes in the 'grey' module were not classified into any modules, so we did not analyze this module. For all 15,481 genes, we used a heatmap to show the weighted network, adjacency relation and topological overlay. In the gene topology, the shade of the color represents the strength of the adjacency. The darker the color is, the stronger the relationship (Fig. 1(A) and (B)). To show the relationships of modules and brain traits, we recalculated a correlation matrix for the module genes. Then, we obtained eigengene adjacency heatmap and dendrogram of six modules for each group. The eigengene adjacency heatmap (Fig. 1(C)) also shows that the yellow and turquoise modules had high adjacency. We found that these six modules were classified into two main clusters (Fig. 1(E)): for the MCI_S group, one included four modules (green, yellow, blue and turquoise), and the other included two modules (brown and red). For the MCI_AD group, the eigengene adjacency heatmap (Fig. 1(D)) also showed that the blue, brown and green modules had high adjacency. We found that these six modules were classified into two main clusters (Fig. 1(F)): one included four modules (green, turquoise, blue and brown), and the other included two modules (red and yellow).

As shown in Fig. 2(A), the 'blue' module had the highest correlation with the thickness value of the L.PTS ($r = 0.3$, $p = 3*10^{-4}$). The 'blue'
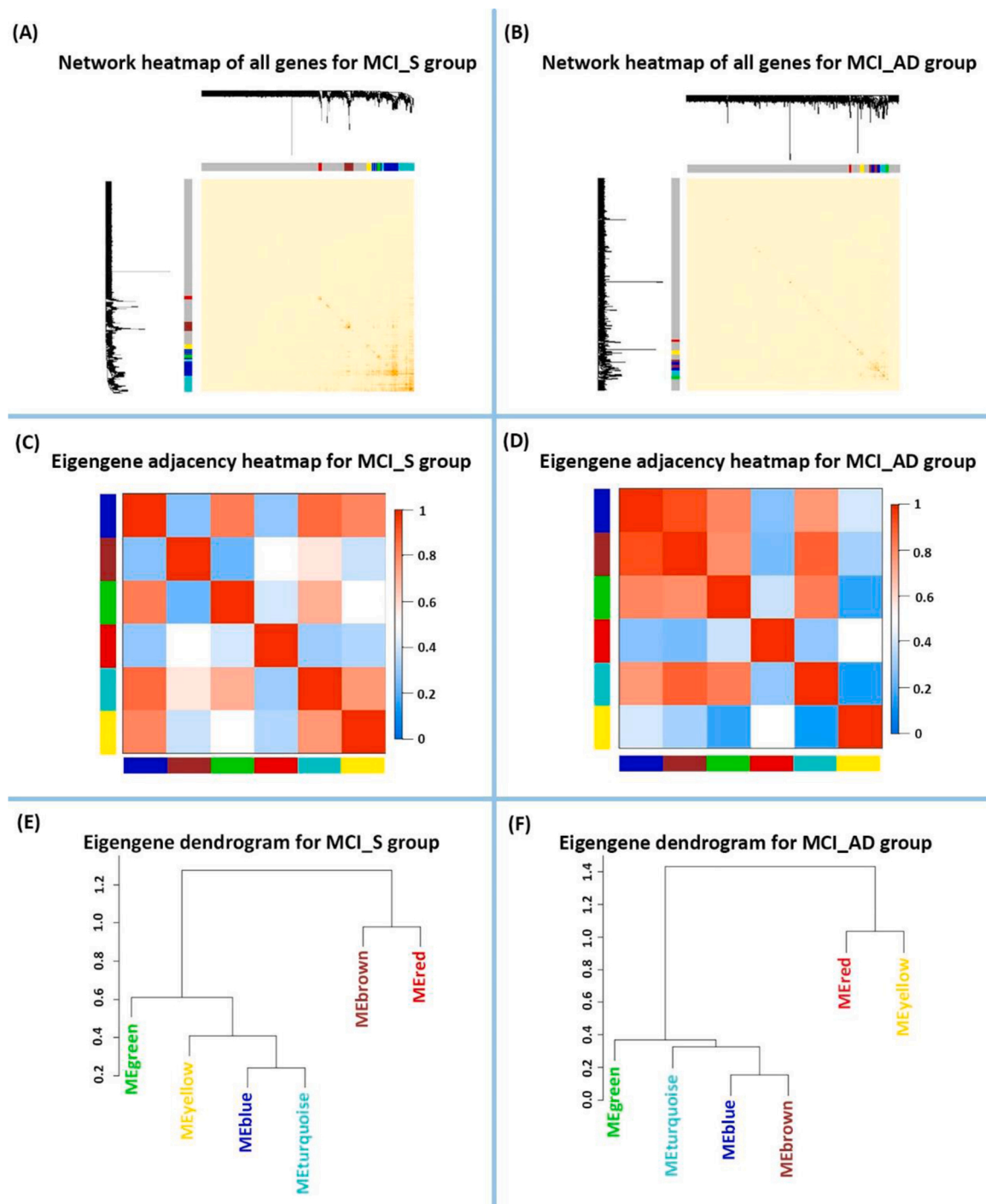
Fig. 1. DEGs and the differentially brain regions in the MCI_S and MCI_AD groups from WGCNA. (A) Network heatmap of all genes in the MCI_S group; (B) Network heatmap of all genes in the MCI_AD group; (C) eigengene adjacency heatmap of six modules in the MCI_S group; (D) eigengene adjacency heatmap of six modules in the MCI_AD group; (E) eigengene dendrogram of six modules in the MCI_S group; (F) eigengene dendrogram of six modules in the MCI_AD group.

module included 60 genes. As shown in Fig. 2(B), the 'turquoise' module had the highest correlation with the thickness of the R.SubPS ($r = 0.45$, $p = 5*10^{-3}$). The 'turquoise' module included 18 genes. Fourteen mutual genes were in these two most correlated modules. Seventy-eight gene IDs, symbols, and descriptions are shown in Supplementary Table S2.

3.4. Enrichment analysis results

According to the enrichment analysis, we found that these genes were mainly involved in muscle structure development, the positive

regulation of I-kappaB kinase/NF-kappaB signaling, base excision repair, endoplasmic reticulum (ER) calcium ion homeostasis and AD. These two groups of genes were also enriched in the same KEGG pathway: AD. Detailed information is shown in Fig. 3.

3.5. Identification of hub genes

Based on the criteria ($|MM|>0.8$ and $|GS|>0.2$), 8 genes in the MCI_S group with high connectivity in the 'blue' module and 5 genes in the MCI_AD group with high connectivity in the 'turquoise' module were
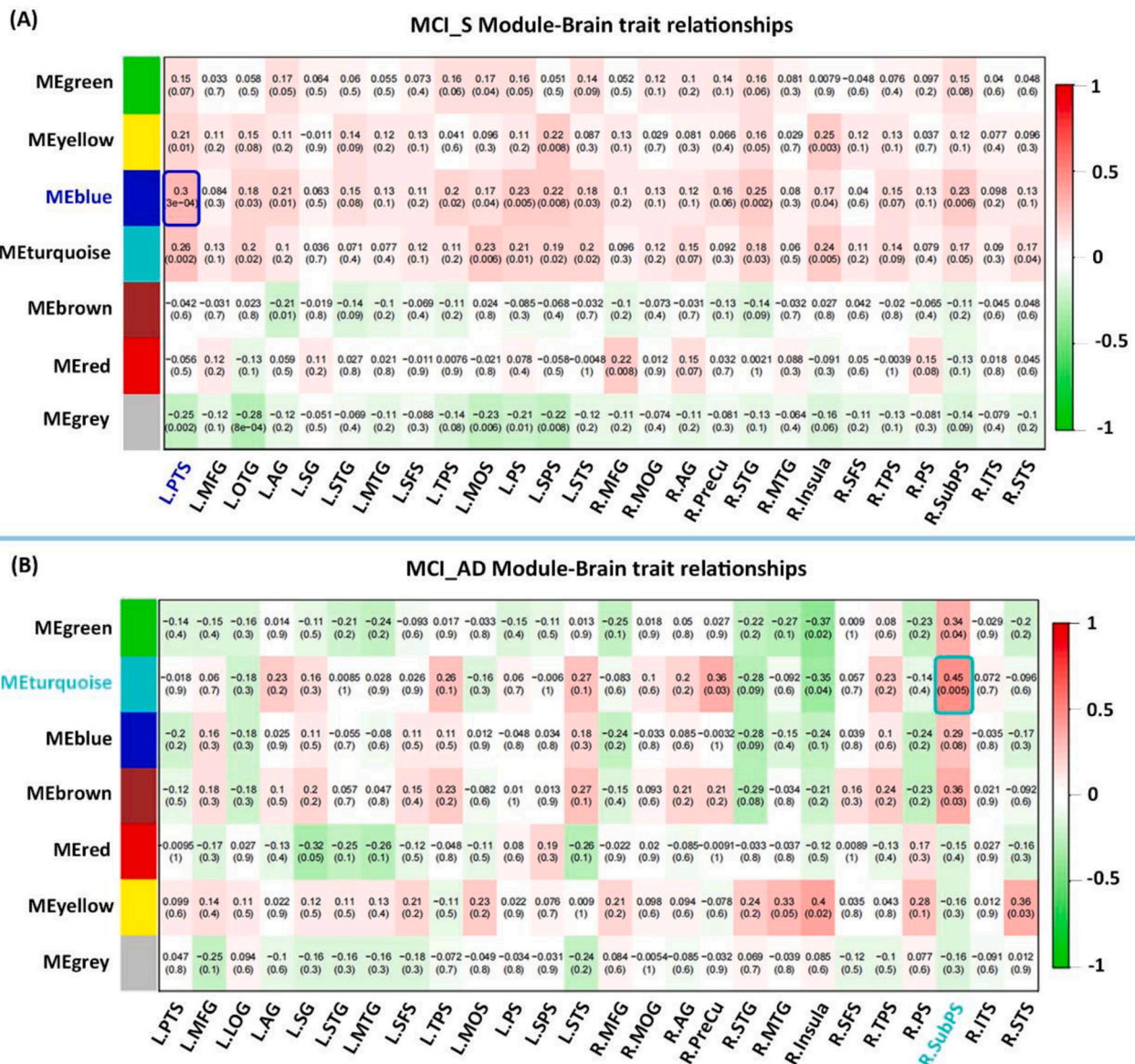
Fig. 2. Module and trait relationships diagram (p < 0.01, FDR correction). (A) Module and brain trait relationships in the MCI_S group. L.PTS: thickness of the left paracentral lobule and sulcus; (B) Module and brain trait relationships in the MCI_AD group. R.SubPS: thickness of the right subparietal sulcus. The remaining abbreviations of the abovementioned brain regions are shown in Supplementary Table S1.

identified as hub genes. Among them, the CTCF, UQCR11 and WDR5B genes were common three genes between MCI_S group and MCI_AD groups. Detail information on these hub genes and the MM values and GS values of all these genes are provided in Supplementary Table S2.

3.6. Correlation analysis results

After the identification, we selected the three common hub genes (CTCF, UQCR11 and WDR5B) between both groups. Then we extracted the gene expression value and the brain measures (cortical thickness of the L.PTS and R.SubPS) and clinical scores. Pearson correlation analysis was aimed at determining whether the brain measures are associated with the expression values and clinical scores of the three hub genes. We found that these three genes were significantly correlated with the L. PTS: 10,664 (CTCF, $r = 0.235$, $p=0.001$), 10,975 (UQCR11, $r=-0.167$, $p=0.025$), and 54,554 (WDR5B, $r=-0.204$, $p=0.006$) but not with the R. SubPS. Then, we performed Pearson correlation analysis between the cortical thickness of the L.PTS and clinical scores. We found that the MMSE, ADAS, ADNI_MEM, ADNI_EF, ADNI_LAN and FAQ scores were

significantly corrected with the cortical thickness of the L.PTS. The aggregated information is shown in Fig. 4.

3.7. Regulating mediator effects analysis

Mediating effect analysis results showed that the cortical thickness of the L.PTS acts as a complete mediator between gene expression (CTCF and UQCR11) and clinical scores (MMSE, ADAS, ADNI_MEM and ADNI_EF) (Fig. 5 and Table 2). The cortical thickness of the L.PTS does not act as a mediator between WDR5B expression and clinical scores. Then, we analyzed whether each mediating effect pathway in Table 2 was regulated by the other two genes. The results of the regulating mediating effect analysis showed that the different expression levels of the UQCR11 and WDR5B genes significantly regulated the mediating effect pathway involved in the CTCF gene. In the pathway of CTCF => thickness of the L.PTS => MMSE (or ADNI_EF) score, when the expression of the WDR5B gene was at low or average level, CTCF gene expression affected the cortical thickness of the L.PTS; when the expression of the UQCR11 gene was at high or average level, the
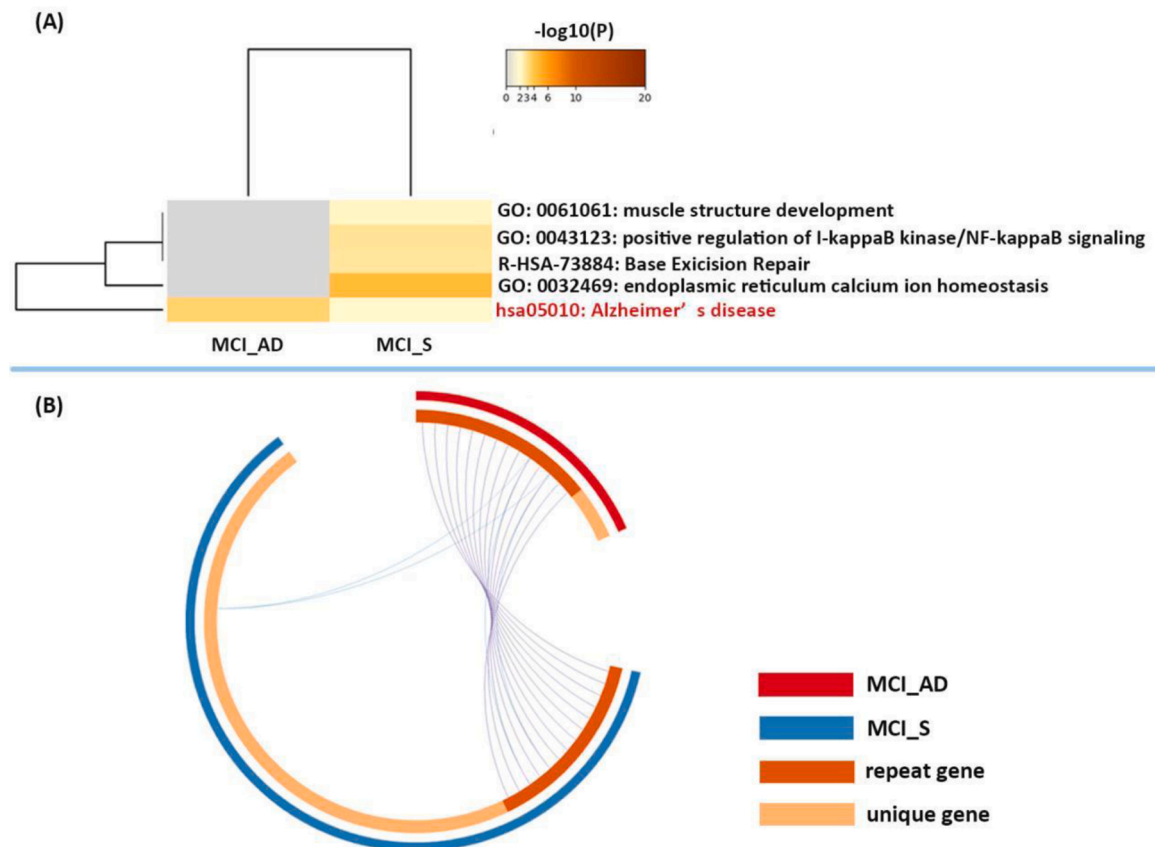
Fig. 3. Enrichment analysis results. (A)Heatmap of enriched terms across input genes, colored by p-values. (B) Overlap between genes. Purple curves link identical genes; blue curves link genes that belong to the same enriched ontology term.

thickness of L.PTS affected the MMSE (or ADNI_EF) score; and when the expression of the WDR5B gene was at low or average level, the thickness of the L.PTS affected the ADNI_EF score. In the pathway of CTCF => thickness of the L.PTS => ADAS (or ADNI_MEM) score, when the expression of the WDR5B gene was at low or average level, CTCF gene expression affected the cortical thickness of the L.PTS; when the expression of the WDR5B or UQCR11 gene was at any level, the thickness of the L.PTS did not affect the ADAS (or ADNI_MEM) score. The mediating effect pathway in UQCR11 is shown in Supplementary Fig. S3 and Supplementary Table S3.

4. Discussion

To preliminarily explore the effects of factors of imaging genetics on conversion from MCI to AD, we applied WGCNA to investigate the associations between 15,481 gene expression and 1,036 brain characteristics of MCI patients who experienced different conversions. We found that 1) 26 brain characteristics and 649 gene expression values were significantly different between the MCI_S and MCI_AD groups; 2) 60 gene expression values had the most significant correlations with the cortical thickness of the L.PTS in the MCI_S group and 18 gene expression values had the most significant correlations with the cortical thickness of the R.SubPS in the MCI_AD group; 3) CTCF, UQCR11, and WDR5B are the mutual genes in MCI_S and MCI_AD groups; and 4) the expression levels of the WDR5B and UQCR11 genes significantly regulate the mediating effect of the CTCF gene. Our results imply that the factors of affecting the conversion of some cases from MCI to AD are closely related to the thickness of the L.PTS and expression levels of the CTCF, UQCR11 and WDR5B genes over the course of the disease.

Several studies have demonstrated that cortical thickness is one of the most sensitive biomarkers for AD, as is structural atrophy [5,11,24].

As the disease progresses from MCI to AD, a general thinning of the entire cortex, including the parietal lobe, frontal lobe, medial temporal lobe, is observed [24,25]. In this study, we identified 26 significantly different characteristics associated with cortical thickness, such as the cortical thicknesses of the superior temporal sulcus, superior frontal sulcus and middle frontal gyrus. Previous studies have noted the importance of frontal lobe and temporal lobe in AD, which is consistent with our findings [26–29]. These changes in cortical thickness may be one of the factors that partially affect conversion from MCI to AD. For gene expression, we found 649 significantly different DEGs between the MCI_S and MCI_AD groups. Berchtold et al. [30], have reported that brain-related gene expression patterns could differentiate MCI from normal aging and AD. The enrichment analysis showed that 649 DEGs were involved in phosphatidylinositol 3-kinase signaling, cellular senescence, synaptic signaling, ion homeostasis and so on. Castri et al., [31] found that the phosphatidylinositol 3-kinase pathway plays an important role in the pathogenesis of AD. LDL receptor-related protein 6 (LRP6) is an essential coreceptor for wnt signaling, and its genetic variants have been linked to AD risk [32]. Sortilin-related VPS10 domain-containing receptor 3 (SORCS3) encodes a type-1 receptor transmembrane protein whose genetic variation is also associated with an increased risk of AD [33,34]. In addition, growth hormone releasing hormone (GHRH) promotes increased circulating levels of insulin-like growth factor 1 (IGF-1) [35]. A prior study suggested that a decreased serum IGF-1 level plays a role as an independent risk factor for AD [36]. This evidence suggests that most of these GO biological processes are related to the pathology of AD [37–39].

Sixty genes had the most significant correlations with the cortical thickness of the L.PTS in the MCI_S group, and 18 genes in the turquoise module had the most significant correlations with the cortical thickness of the R.SubPS in the MCI_AD group. The enrichment analysis
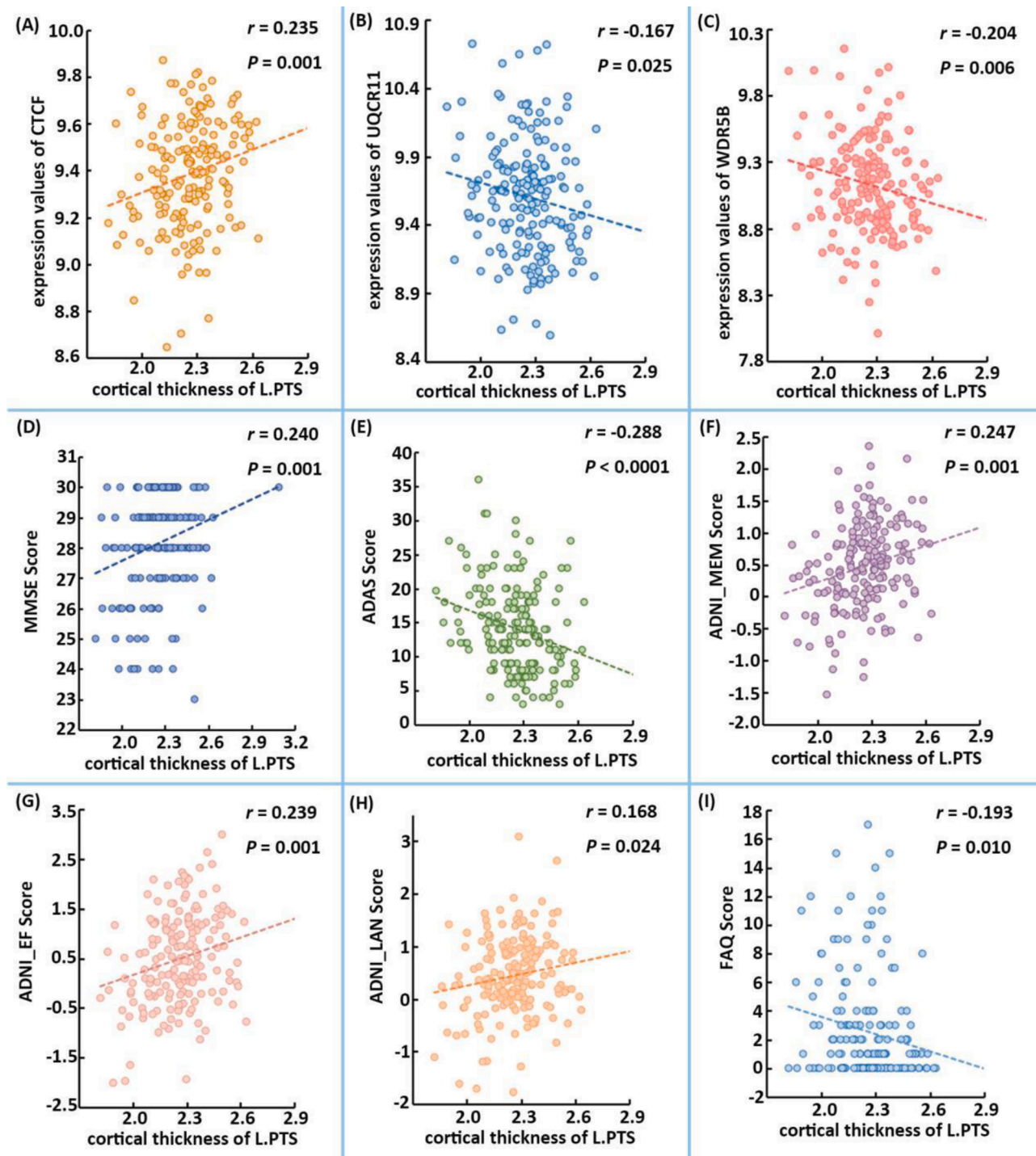
Fig. 4. The Pearson correlations between gene expression, clinical scores and the thickness of the L.PTS. (A) Pearson correlation between the gene expression value of CTCF and cortical thickness of the L.PTS; (B) Pearson correlation between the gene expression values of UQCR11 and cortical thickness of the L.PTS; (C) Pearson correlation between the gene expression values of WDR5B and cortical thickness of the L.PTS; (D) Pearson correlation between cortical thickness of the L.PTS and MMSE score; (E) Pearson correlation between cortical thickness of the L.PTS and ADAS score; (F) Pearson correlation between cortical thickness of the L.PTS and ADNI_MEM score; (G) Pearson correlation between cortical thickness of the L.PTS and ADNI_EF score; (H) Pearson correlation between cortical thickness of the L.PTS and ADNI_LAN score; (I) Pearson correlation between cortical thickness of the L.PTS and FAQ score; **: $p < 0.01$; *: $p < 0.05$.

demonstrated that these genes were mainly involved in ER calcium ion homeostasis. These two groups of genes were also enriched in the same KEGG pathway: AD. These Go biological processes and KEGG pathways play critical roles in the pathology of AD. Calcium cations regulate neuronal plasticity underlying learning and memory and neuronal survival [40]. The ER is an organelle that actively removes calcium ions from the cytoplasm, and previous findings have suggested that

perturbed ER calcium ion homeostasis contributes to the dysfunction and degeneration of neurons observed in AD [41,42]. Our results suggest that changes in gene expression may influence changes in the cortical thickness of the L.PTS and R.SubPS, and then indirectly induce conversion from MCI to AD. Wee et al. [43], found that changes in the paracentral lobule and superior and inferior parietal cortices can be extensively used for the accurate detection of AD or MCI. Yang et al.
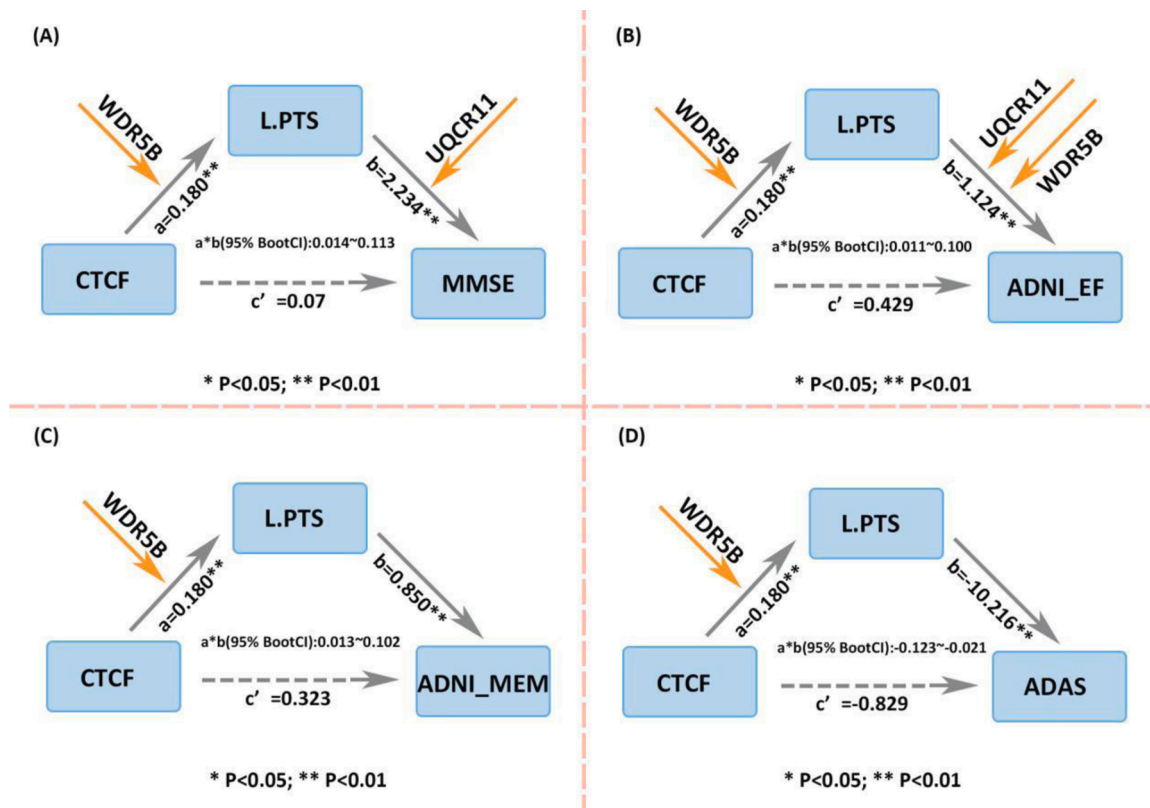
Fig. 5. Regulating mediator effects analysis (A-D): The cortical thickness of L.PTS acts as a complete mediator effect between gene expression values and clinical scores. (A) and (B) the different expression level of the WDR5B and UQCR11 gene significantly regulates the mediating effect pathway involved in CTCF gene, which is in pathway of CTCF => thickness of the L.PTS and thickness of the L.PTS => MMSE (or ADNI_EF) score; (C) and (D) the different expression level of the WDR5B and UQCR11 gene significantly regulates the mediating effect pathway involved in CTCF gene, which is in pathway of CTCF => thickness of the L.PTS. Detailed information is shown in Supplementary Table S3.

Table 2
Mediating effect analysis results.

Mediating effect path	c Total effect	a	b	a*b	a*b (95% BootCI)	c' Direct effect	Testing conclusion
CTCT=>L.PTS=>MMSE	0.472	0.180**	2.234**	0.401	0.014 ~ 0.113	0.07	Complete mediating effect
CTCT=>L.PTS=>ADAS	−2.665	0.180**	−10.216**	−1.836	−0.123 ~ -0.021	−0.829	Complete mediating effect
CTCF =>L.PTS=>ADNI_MEM	0.476*	0.180**	0.850**	0.153	0.013 ~ 0.102	0.323	Complete mediating effect
CTCF =>L.PTS=>ADNI_EF	0.632*	0.180**	1.124**	0.202	0.011 ~ 0.100	0.429	Complete mediating effect

** $p < 0.01$.
* $p < 0.05$. Please refer to the Table 1 and Supplementary Table S1 for all the abbreviations.

[44], found that the cortical thickness of the paracentral lobule was significantly reduced in patients with AD compared with those with MCI. However, there are few studies on the cortical thickness of the subparietal sulcus (SubPS). We aimed to illustrate its adjacent structure. The SubPS provides the lower boundary of the precuneus (PreCu), which is a region of the posteromedial parietal lobe. Its functions include visuospatial imagery, episodic memory retrieval and self-processing operations and consciousness [45]. Csukly et al. [46], found that the PreCu was significantly decreased in amnestic MCI patients relative to healthy controls. Karas et al. [47], found that early-onset AD patients showed disproportionate PreCu atrophy compared to late-onset AD patients. Ye et al., [48] found that the early MCI group exhibited cortical thinning in the left medial temporal region compared with controls, whereas the late MCI group showed cortical thinning in widespread regions, including the medial temporal region and the precuneus. Chen et al. [49], found that the precuneus-based degeneration patterns could aid in the understanding in the neural pathological lesions present in pre-clinical AD patients. Their results indirectly validated our result of morphologic changes in the SubPS.

Interestingly, CTCF, UQCR11 and WDR5B were the mutually expressed in the MCI_S and MCI_AD groups. CTCF is a zinc finger protein, and its mediated gene is involved in the regulation of remote long-term memory in the cortex [50,51]. Mutations in CTCF-binding sites are associated with frontotemporal lobar degeneration, which belongs to the group of neurodegenerative diseases, a single nucleotide polymorphism (SNP) in a CTCF-binding site modifies the surrounding chromatin conformation and spatially regulates the expression level of a causative gene of transmembrane protein 106B (TMEM106B), leading to neuronal death [52]. Augustin et al. [53], identified that CTCF as the binding site of the transcription factor (TF) family that could provide potential targets for the therapeutic treatment of AD by using bioinformatics analysis. UQCR11 encodes the smallest known component of the ubiquinol-cytochrome c reductase complex, which forms part of the mitochondrial respiratory chain. Mitochondrial bioenergetic function, specifically respiratory chain activity [54], is reduced in AD. Armand-Ugon et al. [55], found that UQCR11 expression was decreased in the entorhinal cortex with the development of AD. WDR5B encodes a protein containing several WD40 repeats. The WD40 repeats, as the top

ten most abundant domains in eukaryotes, participate in signal transduction, transcriptional regulation, autophagy, apoptosis and so on [56, 57]. Increasing evidence indicates that dysregulated autophagy plays a key role in the pathogenesis of AD and that macro-autophagy is extensively involved in the neurodegenerative process in AD [58]. Taken together, these results suggest that the CTCF, UQCR11 and WDR5B genes play critical roles in conversion from MCI to AD. For the correlation analysis, the gene expression value of CTCF had a significant negative correlation with the cortical thickness of the L.PTS. However, the gene expression values of UQCR11 and WDR5B had significant positive correlations with the cortical thickness of the L.PTS. This finding means that the lower the expression of CTCF is or the higher the expression of UQCR11 and WDR5B is, the thicker the cortical thickness of the L.PTS. Moreover, the cortical thickness of the L.PTS had a significant positive correlation with the clinical scores (MMSE, memory, executive and language function). The ADAS and FAQ scores had a significant negative correlation with the cortical thickness of the L.PTS. This finding means that the thicker the L.PTS, the better the clinical performance (i.e., higher MMSE, memory, executive, and language function and lower ADAS and FAQ scores). In the early stages of the disease, both cortical thickness and gene expression are quietly changing, underlying the groundwork for conversion from MCI to AD.

The expression value of the CTCF gene and clinical scores were completely mediated by the thickness of the L.PTS. This result implied that the changes of the CTCF gene expression levels affect the thickness of the L.PTS, which ultimately lead to the clinical scores. We found no direct effects of CTCF gene expression on cognition and strong indirect effects of CTCF gene expression on cognition through the thickness of the L.PTS, suggesting that the observed associations of CTCF gene expression on cognition are completely attributable to gene expression effect on cortical atrophy. These findings suggest that high gene expression values promote thinning of the cortex, which, in turn, drives a decline in cognitive performance. A previous study showed that genetic factors contribute to cortical changes throughout life [59]. According to the results of regulating mediating effect analysis, the different expression levels of the UQCR11 and WDR5B genes significantly regulate the mediating effect pathway involved in the CTCF genes. These results indicate that intervening with genetic factors might be the key to preventing the occurrence of AD [60]. In the pathway of CTCF => thickness of the L.PTS => MMSE (or ADNI_EF) score, the WDR5B gene regulates the mediating effect in the subpath of CTCF => thickness of the L.PTS; the UQCR11 and WDR5B gene regulates the subpath of thickness of the L.PTS => MMSE (or ADNI_EF) score. In the pathway of CTCF => thickness of the L.PTS => ADAS (or ADNI_MEM) score, the WDR5B gene regulates the mediating effect in the subpath of CTCF => thickness of the L.PTS but does not regulate the mediating effect in the subpath of thickness of the L.PTS => ADAS (or ADNI_MEM) score. Based on the functional analysis of the three genes, we can infer that the level of ploygene expression affects cortical thickness and hence clinical performance.

Several limitations should be noted. First, in this study, we found that the cortical thickness of the L.PTS is a mediator between the three genes expression and clinical features in conversion from MCI to AD; however, the specific regulatory mechanism still needs further study. Second, the FreeSurfer software package has certain limitations, and its measurement results may be inconsistent [61]. Third, WGCNA does not indicate which co-expression module detection method is best. While the default hierarchical clustering methods have performed well in several real data applications, it would be desirable to use these methods to evaluate our data set and compare the results.

5. Conclusion

We applied WGCNA to investigate the relationships between 15,481 gene expression and 1,036 brain characteristics of MCI patients who experienced different conversions and to explore the imaging genetics

factors for conversion from MCI to AD. We found that the cortical thickness of the L.PTS is a mediator between CTCF, UQCR11 and WDR5B gene expression and clinical features in conversion from MCI to AD. This association indicates that conversion from MCI to AD is closely related to the cortical thickness of the L.PTS and the expression of these three genes. Our study lays an imaging genetics theoretical foundation for the early clinical diagnosis of AD.

Author statement

Xuwen Wang and Suping Cai collected the data, wrote the protocol and designed the whole study together. Liyu Huang supervised the entire project. Kexin Huang and Fan Yang undertook the experimental procedures and analyses. Dihui Chen performed the statistical analysis. All the authors contributed to and have approved the final manuscript.

Declaration of Competing Interest

The authors have no conflicts of interest to declare.

Appendix A. Supplementary data

Supplementary material related to this article can be found, in the online version, at doi:https://doi.org/10.1016/j.bbr.2021.113330.

References

[1] L. Raz, J. Knoefel, K. Bhaskar, The neuropathology and cerebrovascular mechanisms of dementia, J. Cereb. Blood Flow Metabol. 36 (1) (2016) 172–186.

[2] V.V. Giau, E. Bagyinszky, S.S.A. An, Potential fluid biomarkers for the diagnosis of mild cognitive impairment, Int. J. Mol. Sci. 20 (17) (2019).

[3] A.J. Mitchell, M. Shiri-Feshki, Rate of progression of mild cognitive impairment to dementia–meta-analysis of 41 robust inception cohort studies, Acta Psychiatr. Scand. 119 (4) (2009) 252–265.

[4] S. Chaudhury, K.J. Brookes, T. Patel, A. Fallows, T. Guetta-Baranes, J.C. Turton, R. Guerreiro, J. Bras, J. Hardy, P.T. Francis, R. Croucher, C. Holmes, K. Morgan, A. J. Thomas, Alzheimer's disease polygenic risk score as a predictor of conversion from mild-cognitive impairment, Transl. Psychiatry 9 (1) (2019) 154.

[5] L. Sorensen, C. Igel, A. Pai, I. Balas, C. Anker, M. Lillholm, M. Nielsen, I. Alzheimer's Disease Neuroimaging, B. the Australian Imaging, a, Lifestyle flagship study of, Differential diagnosis of mild cognitive impairment and Alzheimer's disease using structural MRI cortical thickness, hippocampal shape, hippocampal texture, and volumetry, Neuroimage Clin. 13 (2017) 470–482.

[6] K. Reiter, K.A. Nielson, T.J. Smith, L.R. Weiss, A.J. Alfini, J.C. Smith, Improved cardiorespiratory fitness is associated with increased cortical thickness in mild cognitive impairment, J. Int. Neuropsychol. Soc. 21 (10) (2015) 757–767.

[7] C.M. Karch, A.M. Goate, Alzheimer's disease risk genes and mechanisms of disease pathogenesis, Biol. Psychiatry 77 (1) (2015) 43–51.

[8] Y. Yang, W.W. Quitschke, A.A. Vostrov, G.J. Brewer, CTCF is essential for up-regulating expression from the amyloid precursor protein promoter during differentiation of primary hippocampal neurons, J. Neurochem. 73 (6) (1999) 2286–2298.

[9] W. Liu, M. Li, W. Zhang, G. Zhou, X. Wu, J. Wang, Q. Lu, H. Zhao, Leveraging functional annotation to identify genes associated with complex diseases, PLoS Comput. Biol. 16 (11) (2020), e1008315.

[10] J.C. Lambert, C.A. Ibrahim-Verbaas, D. Harold, A.C. Naj, Meta-analysis of 74,046 individuals identifies 11 new susceptibility loci for Alzheimer's disease, Nat. Genet. 45 (12) (2013) 1452–1458.

[11] B.H. Kim, Y.H. Choi, J.J. Yang, S. Kim, K. Nho, J.M. Lee, Identification of novel genes associated with cortical thickness in Alzheimer's disease: systems biology approach to neuroimaging endophenotype, J. Alzheimers Dis. 75 (2) (2020) 531–545.

[12] P. Langfelder, S. Horvath, WGCNA: an R package for weighted correlation network analysis, BMC Bioinformatics 9 (2008) 559.

[13] S. Mukherjee, C. Klaus, M. Pricop-Jeckstadt, J.A. Miller, F.L. Struebing, A microglial signature directing human aging and neurodegeneration-related gene networks, Front. Neurosci. 13 (2019) 2.

[14] J.W. Liang, Z.Y. Fang, Y. Huang, Z.Y. Liuyang, X.L. Zhang, J.L. Wang, H. Wei, J. Z. Wang, X.C. Wang, J. Zeng, R. Liu, Application of weighted gene co-expression network analysis to explore the key genes in Alzheimer's disease, J. Alzheimers Dis. 65 (4) (2018) 1353–1364.

[15] Y. Sun, J. Lin, L. Zhang, The application of weighted gene co-expression network analysis in identifying key modules and hub genes associated with disease status in Alzheimer's disease, Ann. Transl. Med. 7 (24) (2019) 800.

[16] Z.T. Wang, C.C. Tan, L. Tan, J.T. Yu, Systems biology and gene networks in Alzheimer's disease, Neurosci. Biobehav. Rev. 96 (2019) 31–44.

[17] N.S. Soleimani Zakeri, S. Pashazadeh, H. MotieGhader, Gene biomarker discovery at different stages of Alzheimer using gene co-expression network approach, Sci. Rep. 10 (1) (2020) 12210.

[18] K. Sato, T. Mano, H. Matsuda, M. Senda, R. Ihara, K. Suzuki, H. Arai, K. Ishii, K. Ito, T. Ikeuchi, R. Kuwano, T. Toda, T. Iwatsubo, A. Iwata, I. Japanese Alzheimer's Disease Neuroimaging, Visualizing modules of coordinated structural brain atrophy during the course of conversion to Alzheimer's disease by applying methodology from gene co-expression analysis, Neuroimage Clin. 24 (2019), 101957.

[19] J.D. Blumenthal, A. Zijdenbos, E. Molloy, J.N. Giedd, Motion artifact in magnetic resonance imaging: implications for automated analysis, Neuroimage 16 (1) (2002) 89–92.

[20] H.R. Pardoe, R. Kucharsky Hiess, R. Kuzniecky, Motion and morphometry in clinical and nonclinical populations, Neuroimage 135 (2016) 177–185.

[21] K.J. Gorgolewski, F. Alfaro-Almagro, T. Auer, P. Bellec, M. Capotă, M. M. Chakravarty, N.W. Churchill, A.L. Cohen, R.C. Craddock, G.A. Devenyi, BIDS apps: improving ease of use, accessibility, and reproducibility of neuroimaging data analysis methods, PLoS Comput. Biol. 13 (3) (2017), e1005209.

[22] S. Cai, Y. Jiang, Y. Wang, X. Wu, J. Ren, M.S. Lee, S. Lee, L. Huang, Modulation on brain gray matter activity and white matter integrity by APOE ε4 risk gene in cognitively intact elderly: a multimodal neuroimaging study, Behav. Brain Res. 322 (2017) 100–109.

[23] Zhou Yingyao, Lars Bin, Max Pache, Alireza Chang, Khodabakhshi Hadj, Metascape provides a biologist-oriented resource for the analysis of systems-level datasets, Nat. Commun. (2019).

[24] V. Singh, H. Chertkow, J.P. Lerch, A.C. Evans, A.E. Dorr, N.J. Kabani, Spatial patterns of cortical thinning in mild cognitive impairment and Alzheimer's disease, Brain 129 (Pt 11) (2006) 2885–2893.

[25] A.M. Kälin, M.T. Park, M.M. Chakravarty, J.P. Lerch, L. Michels, C. Schroeder, S. D. Broicher, S. Kollias, R.M. Nitsch, A.F. Gietl, P.G. Unschuld, C. Hock, S.E. Leh, Subcortical shape changes, hippocampal atrophy and cortical thinning in future Alzheimer's disease patients, Front. Aging Neurosci. 9 (2017) 38.

[26] B.C. Dickerson, E. Feczko, J.C. Augustinack, J. Pacheco, J.C. Morris, B. Fischl, R. L. Buckner, Differential effects of aging and Alzheimer's disease on medial temporal lobe cortical thickness and surface area, Neurobiol. Aging 30 (3) (2009) 432–440.

[27] A.T. Du, N. Schuff, J.H. Kramer, H.J. Rosen, M.L. Gorno-Tempini, K. Rankin, B. L. Miller, M.W. Weiner, Different regional patterns of cortical thinning in Alzheimer's disease and frontotemporal dementia, Brain 130 (Pt 4) (2007) 1159–1166.

[28] P. Hartikainen, J. Räsänen, V. Julkunen, E. Niskanen, M. Hallikainen, M. Kivipelto, R. Vanninen, A.M. Remes, H. Soininen, Cortical thickness in frontotemporal dementia, mild cognitive impairment, and Alzheimer's disease, J. Alzheimer's Dis. 30 (4) (2012) 857–874.

[29] C. Li, J. Wang, L. Gui, J. Zheng, C. Liu, H. Du, Alterations of whole-brain cortical area and thickness in mild cognitive impairment and Alzheimer's disease, J. Alzheimer's Dis. 27 (2) (2011) 281–290.

[30] N.C. Berchtold, M.N. Sabbagh, T.G. Beach, R.C. Kim, D.H. Cribbs, C.W. Cotman, Brain gene expression patterns differentiate mild cognitive impairment from normal aged and Alzheimer's disease, Neurobiol. Aging 35 (9) (2014) 1961–1972.

[31] P. Castri, L. Iacovelli, A. De Blasi, F. Giubilei, A. Moretti, F. Tari Capone, F. Nicoletti, F. Orzi, Reduced insulin-induced phosphatidylinositol-3-kinase activation in peripheral blood mononuclear leucocytes from patients with Alzheimer's disease, Eur. J. Neurosci. 26 (9) (2007) 2469–2472.

[32] C.C. Liu, C.W. Tsai, F. Deak, J. Rogers, M. Penuliar, Y.M. Sung, J.N. Maher, Y. Fu, X. Li, H. Xu, S. Estus, H.S. Hoe, J.D. Fryer, T. Kanekiyo, G. Bu, Deficiency in LRP6-mediated Wnt signaling contributes to synaptic abnormalities and amyloid pathology in Alzheimer's disease, Neuron 84 (1) (2014) 63–77.

[33] C. Reitz, The role of the retromer complex in aging-related neurodegeneration: a molecular and genomic review, Mol. Genet. Genomics: MGG 290 (2) (2015) 413–427.

[34] C. Reitz, G. Tosto, B. Vardarajan, E. Rogaeva, M. Ghani, R.S. Rogers, C. Conrad, J. L. Haines, M.A. Pericak-Vance, M.D. Fallin, T. Foroud, L.A. Farrer, G. D. Schellenberg, P.S. George-Hyslop, R. Mayeux, Independent and epistatic effects of variants in VPS10-d receptors on Alzheimer disease risk and processing of the amyloid precursor protein (APP), Transl. Psychiatry 3 (5) (2013) e256.

[35] C.N. Winston, E.J. Goetzl, L.D. Baker, M.V. Vitiello, R.A. Rissman, Growth hormone-releasing hormone modulation of neuronal exosome biomarkers in mild cognitive impairment, J. Alzheimer's Dis. 66 (3) (2018) 971–981.

[36] T. Watanabe, A. Miyazaki, T. Katagiri, H. Yamamoto, T. Idei, T. Iguchi, Relationship between serum insulin-like growth factor-1 levels and Alzheimer's disease and vascular dementia, J. Am. Geriatr. Soc. 53 (10) (2005) 1748–1753.

[37] P.H. Reddy, J. Williams, F. Smith, J.S. Bhatti, S. Kumar, M. Vijayan, R. Kandimalla, C.S. Kuruva, R. Wang, M. Manczak, X. Yin, A.P. Reddy, MicroRNAs, aging, cellular senescence, and Alzheimer's disease, in: Progress in Molecular Biology and Translational Science, 146, 2017, pp. 127–171.

[38] S. Forner, D. Baglietto-Vargas, A.C. Martini, L. Trujillo-Estrada, F.M. LaFerla, Synaptic impairment in Alzheimer's disease: a dysregulated symphony, Trends Neurosci. 40 (6) (2017) 347–357.

[39] L. Wang, Y.L. Yin, X.Z. Liu, P. Shen, Y.G. Zheng, X.R. Lan, C.B. Lu, J.Z. Wang, Current understanding of metal ions in the pathogenesis of Alzheimer's disease, Transl. Neurodegener. 9 (2020) 10.

[40] G. Zündorf, G. Reiser, Calcium dysregulation and homeostasis of neural calcium in the molecular mechanisms of neurodegenerative diseases provide multiple targets for neuroprotection, Antioxid. Redox Signal. 14 (7) (2011) 1275–1288.

[41] M.P. Mattson, ER calcium and Alzheimer's disease: in a state of flux, Sci. Signal. 3 (114) (2010) pe10.

[42] W. Paschen, J. Doutheil, Disturbances of the functioning of endoplasmic reticulum: a key mechanism underlying neuronal cell injury? J. Cereb. Blood Flow Metab. 19 (1) (1999) 1–18.

[43] C.Y. Wee, P.T. Yap, D. Shen, Prediction of Alzheimer's disease and mild cognitive impairment using cortical morphological patterns, Hum. Brain Mapp. 34 (12) (2013) 3411–3425.

[44] H. Yang, H. Xu, Q. Li, Y. Jin, W. Jiang, J. Wang, Y. Wu, W. Li, C. Yang, X. Li, S. Xiao, F. Shi, T. Wang, Study of brain morphology change in Alzheimer's disease and amnestic mild cognitive impairment compared with normal controls, Gen. Psychiatry 32 (2) (2019), e100005.

[45] A.E. Cavanna, M.R. Trimble, The precuneus: a review of its functional anatomy and behavioural correlates, Brain 129 (Pt 3) (2006) 564–583.

[46] G. Csukly, E. Sirály, Z. Fodor, A. Horváth, P. Salacz, Z. Hidasi, É. Csibri, G. Rudas, Á. Szabó, The differentiation of amnestic type MCI from the non-amnestic types by structural MRI, Front. Aging Neurosci. 8 (2016) 52.

[47] G. Karas, P. Scheltens, S. Rombouts, R. van Schijndel, M. Klein, B. Jones, W. van der Flier, H. Vrenken, F. Barkhof, Precuneus atrophy in early-onset Alzheimer's disease: a morphometric structural MRI study, Neuroradiology 49 (12) (2007) 967–976.

[48] B.S. Ye, S.W. Seo, J.J. Yang, H.J. Kim, Y.J. Kim, C.W. Yoon, H. Cho, Y. Noh, G. H. Kim, J. Chin, J.H. Kim, S. Jeon, J.M. Lee, D.L. Na, Comparison of cortical thickness in patients with early-stage versus late-stage amnestic mild cognitive impairment, Eur. J. Neurol. 21 (1) (2014) 86–92.

[49] Y. Chen, Z. Liu, J. Zhang, K. Chen, L. Yao, X. Li, G. Gong, J. Wang, Z. Zhang, Precuneus degeneration in nondemented elderly individuals with APOE ε4: evidence from structural and functional MRI analyses, Hum. Brain Mapp. 38 (1) (2017) 271–282.

[50] S. Kim, N.K. Yu, K.W. Shim, J.I. Kim, H. Kim, D.H. Han, J.E. Choi, S.W. Lee, D. I. Choi, M.W. Kim, D.S. Lee, K. Lee, N. Galjart, Y.S. Lee, J.H. Lee, B.K. Kaang, Remote memory and cortical synaptic plasticity require neuronal CCCTC-Binding factor (CTCF), J. Neurosci. 38 (22) (2018) 5042–5052.

[51] J.E. Phillips, V.G. Corces, CTCF: master weaver of the genome, Cell 137 (7) (2009) 1194–1211.

[52] M. Kikuchi, N. Hara, M. Hasegawa, A. Miyashita, R. Kuwano, T. Ikeuchi, A. Nakaya, Enhancer variants associated with Alzheimer's disease affect gene expression via chromatin looping, BMC Med. Genomics 12 (1) (2019) 128.

[53] R. Augustin, S.F. Lichtenthaler, M. Greeff, J. Hansen, W. Wurst, D. Trumbach, Bioinformatics identification of modules of transcription factor binding sites in Alzheimer's disease-related genes by in silico promoter analysis and microarrays, Int. J. Alzheimers Dis. (2011), 154325, 2011.

[54] E. Area-Gomez, A. de Groof, E. Bonilla, J. Montesinos, K. Tanji, I. Boldogh, L. Pon, E.A. Schon, A key role for MAM in mediating mitochondrial dysfunction in Alzheimer disease, Cell Death Dis. 9 (3) (2018) 335.

[55] M. Armand-Ugon, B. Ansoleaga, S. Berjaoui, I. Ferrer, Reduced mitochondrial activity is early and steady in the entorhinal cortex but it is mainly unmodified in the frontal cortex in Alzheimer's disease, Curr. Alzheimer Res. 14 (12) (2017) 1327–1334.

[56] D. Li, R. Roberts, WD-repeat proteins: structure characteristics, biological function, and their involvement in human diseases, Cell. Mol. Life Sci.: CMLS 58 (14) (2001) 2085–2097.

[57] E.J. Neer, C.J. Schmidt, R. Nambudripad, T.F. Smith, The ancient regulatory-protein family of WD-repeat proteins, Nature 371 (6495) (1994) 297–300.

[58] F. Guo, X. Liu, H. Cai, W. Le, Autophagy in neurodegenerative diseases: pathogenesis and therapy, Brain Pathol. (Zurich, Switzerland) 28 (1) (2018) 3–13.

[59] A.M. Fjell, H. Grydeland, S.K. Krogsrud, I. Amlien, D.A. Rohani, L. Ferschmann, A. B. Storsve, C.K. Tamnes, R. Sala-Llonch, P. Due-Tønnessen, A. Bjørnerud, A. E. Sølsnes, A.K. Håberg, J. Skranes, H. Bartsch, C.H. Chen, W.K. Thompson, M. S. Panizzon, W.S. Kremen, A.M. Dale, K.B. Walhovd, Development and aging of cortical thickness correspond to genetic organization patterns, Proc. Natl. Acad. Sci. U. S. A. 112 (50) (2015) 15462–15467.

[60] M. Robinson, B.Y. Lee, F.T. Hane, Recent progress in Alzheimer's disease research, part 2: genetics and epidemiology, J. Alzheimers Dis. 57 (2) (2017) 317–330.

[61] S.N. Yaakub, R.A. Heckemann, S.S. Keller, C.J. McGinnity, B. Weber, A. Hammers, On brain atlas choice and automatic segmentation methods: a comparison of MAPER & FreeSurfer using three atlas databases, Sci. Rep. 10 (1) (2020) 2837.